Optics Letters

AlGaAs-on-insulator waveguide for highly efficient photon-pair generation via spontaneous four-wave mixing

Hatam Mahmudlu,[1,2,3] Stuart May,[4] Alí Angulo,[1,2,3,6] Marc Sorel,[4,5] and Michael Kues[1,2,3,*]

[1]Institute of Photonics, Leibniz University Hannover, Nienburger Str. 17, 30167 Hannover, Germany
[2]Hannover Centre for Optical Technologies, Leibniz University Hannover, Nienburger Str. 17, 30167 Hannover, Germany
[3]Cluster of Excellence PhoenixD (Photonic, Optics, and Engineering—Innovation Across Disciplines), Leibniz University Hannover, Hannover, Germany
[4]School of Engineering, University of Glasgow, Glasgow G12 8QQ, UK
[5]Institute of Technologies for Communication, Information and Perception (TeCIP), Sant'Anna School of Advanced Studies, Via Moruzzi 1, 56127 Pisa, Italy
[6]e-mail: ali.angulo@hot.uni-hannover.de
*Corresponding author: michael.kues@hot.uni-hannover.de

Received 4 January 2021; revised 25 January 2021; accepted 25 January 2021; posted 27 January 2021 (Doc. ID 418932); published 22 February 2021

We report on the generation of correlated photon pairs in AlGaAs-on-insulator (AlGaAs-OI) waveguides through nonlinear spontaneous four-wave-mixing (SFWM). Our measurements reveal an SFWM pair generation efficiency of ∼0.096 × 10^{12} pairs/(sW^2) at a wavelength of 1550 nm. This is one of the highest efficiencies achieved to date for integrated SFWM sources. A maximal coincidence-to-accidental ratio of ∼122 is measured. A spectral characterization of the device's pair emission at the quantum level demonstrates a broad generation bandwidth of 2.0 THz, which is important for frequency multiplexing applications. Our results indicate that AlGaAs-OI is an efficient material platform for integrated quantum photonics at telecom wavelengths.

https://doi.org/10.1364/OL.418932

Generating high photon-pair rates is critical to create efficient quantum sources for applications such as secure non-classical telecommunication [1], quantum teleportation [2], and quantum information processing [3], which represent major steps toward the development of the quantum internet [4]. Additionally, sources with a broad generation bandwidth are essential for applications in quantum frequency multiplexing [5] and spectral compression to, e.g., address quantum memories [6]. In order to meet today's technology requirements in terms of stability, compactness, and large-volume manufacturability, advances in the development of photon-pair sources in photonic integrated technologies are necessary [7,8]. A broad range of photonic integrated sources have been developed exploiting nonlinear effects in diverse materials such as silicon [7,8], Si_3N_4 [9], As_2S_3 [10], and AlGaAs [11,12]. AlGaAs material platforms have been dubbed the "silicon of nonlinear optics," as they combine mature manufacturing processing with one of the highest nonlinearities of materials commonly used for integrated photonics [13–15]. Furthermore, modifications of the Al concentration in the alloy allow for the reduction of two-photon absorption (TPA) at telecommunication wavelengths, which represents a major advantage over silicon devices [16]. AlGaAs waveguides grown on their native GaAs substrate have shown notable results for photon-pair generation [17]; however, the phase matching condition necessary for nonlinear processes often requires the construction of submicron waveguides, which frequently results in high propagation losses due to the low refractive index differences between AlGaAs layers [18,19]. The fabrication of integrated waveguides with an AlGaAs core on a silica cladding layer, i.e., AlGaAs-on-insulator (AlGaAs-OI), provides a higher refractive index contrast between the guiding medium and the cladding material. This leads to lower propagation losses as well as enhanced effective nonlinearities because of the sub-micrometer modal confinement, thus resulting in a very efficient nonlinear platform [14,20,21]. AlGaAs-OI devices have produced remarkable results in the classical regime: Kerr comb generation [22], dissipative Kerr soliton generation [23], efficient frequency comb generation through FWM [20], broadband supercontinuum generation [24], and the first time realization of all-optical wavelength conversion of 10 Gbaud data signals at sub-milliwatt pump power levels [25]. Moreover, highly efficient second harmonic generation has also been shown in GaAs-OI [26] and AlGaAs-OI [14] waveguides. These results demonstrate the potential to exploit the large nonlinearities of AlGaAs in compact integrated chips. In particular, thanks to low propagation losses and high second-order $\chi^{(2)}$ and third-order $\chi^{(3)}$ nonlinearities, AlGaAs-OI is a very promising

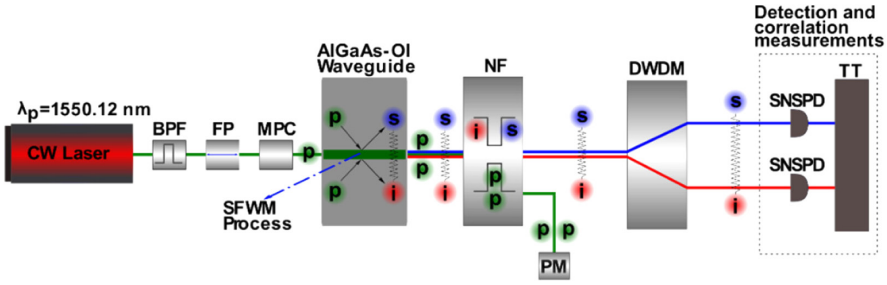

Fig. 1. Experimental setup. A continuous wave (CW) laser centered at $\lambda_p = 1550.12$ nm ($\nu_p = 193.4$ THz) was passed through a fiber high-rejection bandpass filter (BPF) (100 dB) with a 100 GHz bandwidth, suppressing the laser sideband modes. Subsequently, the excitation field was guided into a fiber polarizer (FP). A manual polarization controller (MPC) ensured a TE_{00} waveguide-mode excitation. Through the SFWM process, two input excitation photons with frequency (ω_p) are annihilated, while a pair of signal (ω_s) and idler (ω_i) photons are created. Due to energy ($2\omega_p = \omega_s + \omega_i$) and momentum conservation ($2k_p = k_s + k_i$), the generated photons exhibit correlations in the frequency-time domain and are referred to as quantum-correlated photon pairs [27]. A power meter (PM) measured the excitation field intensity after a notch filter (NF) of 200 GHz isolation bandwidth for separating the excitation signal from the single-photon signal. The signal and idler photons were split with a programmable filter (DWDM) and subsequently detected by two superconducting nanowire single-photon detectors (SNSPD). Their time correlations were determined by a time tagger (TT) in a 5 ps resolution mode. The green, blue, and red circles represent schematically the excitation, signal, and idler photons, respectively.

candidate for highly efficient photon-pair generation via spontaneous parametric down conversion (SPDC) and spontaneous four-wave mixing (SFWM) processes.

In this Letter, we demonstrate the first photon-pair generation via SFWM in a low-loss AlGaAs-OI waveguide. For details on the fabrication method see [24]. The waveguide had a cross-section width of 450 nm, a height of 270 nm, and a length of 3 mm, providing single-mode TE propagation. An aluminum percentage of 30% was chosen for the AlGaAs alloy to avoid TPA at telecom wavelengths. We report an SFWM pair generation efficiency of $a \approx 0.096 \times 10^{12}$ pairs/$(\mathrm{s} \cdot \mathrm{W}^2)$ and a maximal coincidence-to-accidental ratio of ~122 at 1550 nm wavelength. A spectral characterization of the pair emission revealed a large effective generation bandwidth (EGB) of ~2.0 THz.

The pair generation characteristics of our AlGaAs-OI waveguides were characterized using the experimental setup in Fig. 1.

An important characteristic of SFWM quantum sources is the pair generation efficiency a. In order to determine this efficiency, we considered the SFWM coincidence rate μ and the single-photon rates S_s, S_i (here defined at the output of the waveguide) as a function of the excitation power P_{in}. We accounted for noise photons emerging from power-dependent Raman scattering with efficiencies b_s, b_i. The power dependence is described by the following equations [17]:

$$\mu = a\, {P_{\mathrm{in}}}^2, \tag{1}$$

$$S_i = [\mu + b_i P_{\mathrm{in}}], \quad \text{and} \tag{2}$$

$$S_s = [\mu + b_s P_{\mathrm{in}}], \tag{3}$$

where P_{in} is the power inside the waveguide. We performed power-dependent measurements of single and coincidence rates. To extract the generation efficiency, the chip-to-fiber end-fire coupling T_α, experimental setup transmission T_{exp}, and detection efficiencies η_i, η_s needed to be considered. Here, T_α describes the mode-field coupling transmission from the waveguide output facet to the input fiber lens, and it was determined through power-dependent classical measurements (see Table 1). T_{exp} describes the transmission through the rejection arm of the notch filter and the rest of the experimental setup (which was determined by classical measurements). Therefore, the overall transmission is $\zeta = (T_\alpha \cdot T_{\mathrm{exp}})$. Taking this into account, the detected coincidence counts are described by $\mu_d = \zeta^2 \cdot \eta_i \cdot \eta_s \cdot \mu = a_d \cdot P_d^2$. Here, $P_d = \zeta_p \cdot P_{\mathrm{in}}$ is the detected power with $\zeta_p = T_{\mathrm{WG}} \cdot T_\alpha \cdot T_{\mathrm{NF}}$ (where T_{WG} is the waveguide transmission and T_{NF} the transmission through the notch filter). Hence, the pair generation efficiency results in $a = \frac{{\zeta_p}^2 \cdot a_d}{\zeta^2 \cdot \eta_i \cdot \eta_s}$. Accordingly, the detected single counts yield $S_{i,d} = \eta_i \cdot \zeta \cdot S_i$ and $S_{s,d} = \eta_s \cdot \zeta \cdot S_s$. This leads to the following power-dependent relation for the detected parameters:

$$\mu_d = a_d \cdot {P_d}^2, \tag{4}$$

$$S_{i,d} = \frac{a_d}{\zeta \cdot \eta_s} {P_d}^2 + \frac{b_{i,d}}{\zeta_p} P_d, \quad \text{and} \tag{5}$$

$$S_{s,d} = \frac{a_d}{\zeta \cdot \eta_i} {P_d}^2 + \frac{b_{s,d}}{\zeta_p} P_d, \tag{6}$$

where $b_{i,d} = \zeta \cdot \eta_i \cdot b_i$ and $b_{s,d} = \zeta \cdot \eta_s \cdot b_s$ are the detected Raman efficiencies. The detected generation rate μ_d as a function of the detected power P_d is shown in Fig. 2(a). From this, a fit with Eq. (4) allowed the determination of the detected generation efficiency a_d. The detected signal and idler counts as a function of P_d are shown in Fig. 2(b). With a measured propagation loss of 3 dB/cm, using a_d and classically determined transmission values (T_α, T_{NF}, T_{exp}) permitted the acquisition of the detector efficiencies η_s and η_i as well as the detected Raman efficiencies $b_{i,d}$ and $b_{s,d}$ through linear fitting. We obtained an SFWM generation efficiency of $a \approx 0.096 \times 10^{12}$ pairs/$(\mathrm{s} \cdot \mathrm{W}^2)$ which allows for the intrinsic characterization of AlGaAs-OI as a material platform (see Table 1). Compared with other platforms, such as AlGaAs, c-Si, and a-Si (see Table 2), our generation efficiency is one

Table 1. AlGaAs-OI Photon-pair Generation Parameters Obtained from Our Experiments[a]

w	a	b_i	b_s	μ'	η_i	η_s	T_α
450	0.096 ±0.019	1.51 ±0.15	1.41 ±0.14	1.109 ±0.91	0.74	0.87	0.056 ±0.005

[a] a, pair generation efficiency [10^{12} pairs/(s · W^2)]; b_i, b_s, Raman efficiencies [10^{10}counts/(s· W)]; μ', pair generation rate (10^3 pair/s/nm); w, width of the waveguide (nm).

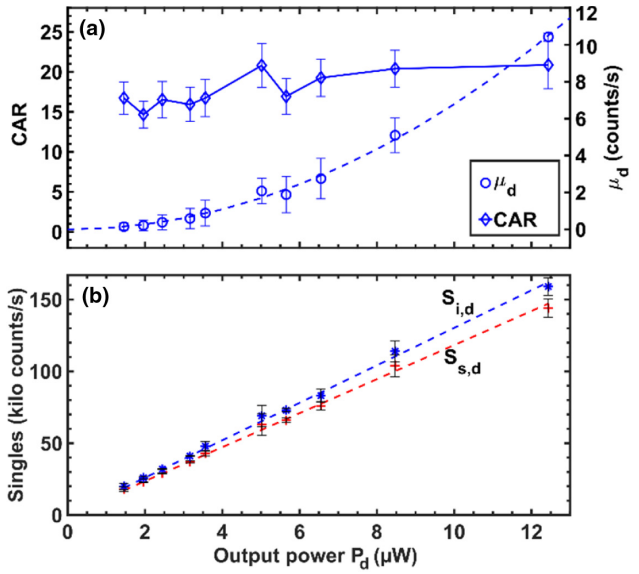

Fig. 2. (a) Measured coincidence rate (μ_d) for the waveguide and fit of the Eq. (4) (dashed lines), as well as the extracted coincidence-to-accidental ratio (CAR) (solid lines are used to guide the eye); (b) measured signal and idler single counts for the waveguide ($S_{s,d}$, $S_{i,d}$) and fit of the Eqs. (5) and (6). ($\lambda_i = 1556.53$ nm, $\lambda_s = 1543.71$ nm).

Table 2. Comparison of SFWM Parameters with Other Structures[a]

Work	AlGaAs-OI	a-Si [28]	c-Si [29]
a	∼0.096	∼0.0009375	∼0.076
CAR	∼21	∼10	∼673
Pairs/s (at P_{in})	∼11,760 (354 μW)	∼2,500 (2 mW)	∼7,600 (1 mW)
Filter BW	10.6	15.5	0.4

[a] pair generation efficiency [10^{12} pairs/(s · W^2)]; BW, bandwidth (nm).

of the highest reported for an integrated SFWM photon-pair source.

The external generation efficiency of this specific device (i.e., the ratio of the detected photon pairs and the input power) is $a_{ext} \approx 0.047 \times 10^6$ pairs/(s · W^2). This parameter strongly depends on the setup conditions and can be enhanced by loss optimization. The intrinsic efficiency value a is not affected and thus represents a good measure for platform comparison.

Considering an input power of $P_{in} = 354$ μW, the coincidence rate per nm at the waveguide output was $\mu' \approx 1.109 \times 10^3$ pair/s/nm. The coincidence-to-accidental ratio (CAR) for a filter bandwidth of 1.3 THz was ∼21 [see Fig. 2(a)]. Although such a CAR is not very high, it can still be readily used in quantum information processing [30]. The current outcoupling loss of our device limits the CAR value. A mode-field converter that reduces the outcoupling loss to, e.g., 3 dB after generation can further improve the CAR to ∼185. Furthermore, for an input power of 8 mW, achievable with further optimization, a coincidence rate of $\mu' \approx 5.7 \times 10^5$ pair/s/nm could be reached. Remarkably, such a coincidence rate is comparable to the ones of previously reported GaAs/AlGaAs sources based on SPDC [31]. Additionally, the extracted Raman coefficients show slightly higher efficiencies for the idler (Stokes) than for the signal (anti-Stokes) (see Table 1). This negligible difference between the coefficients is an indication that the used spectral filter positions are not in the range of the maximum Raman bands [32].

To study the spectral effective generation bandwidth (EGB) of the SFWM process, we performed coincidence measurements while adapting the spectral position of the signal and idler filters with 50 GHz bandwidths symmetric to the excitation frequency. EGB is considered to be twice of the full width at half maximum (FWHM) of the counts as a function of the difference between filter center frequency and excitation frequency. The coincidence rate and CAR as a function of the spectral detuning are shown in Fig. 3(a). The source's pair emission showed a generation over an EGB ≈ 2.0 THz, and the CAR reached a value of ∼120 due to noise filtering [33] with narrower collection filter bandwidth (50 GHz). Additionally, in combination with a mode-field converter that leads to an outcoupling loss of, e.g., 3 dB, the CAR could be increased to ∼1060. Figure 3(b) represents the theoretical wavelength-dependent calculation of the group velocity dispersion (GVD) (β_2) of the waveguide, where the semi-empirical model from Gehrsitz has been assumed for the material dispersion of the AlGaAs core [34]. At the excitation wavelength of 1550 nm, the GVD is anomalous and close to the zero-dispersion wavelength. Theoretical considerations indicate an increase in generation bandwidth [10,35] the closer the excitation wavelength is to the zero-dispersion point. Our study was limited by the passband of the available high-rejection filters.

In conclusion, we have demonstrated the generation of correlated photon pairs from an AlGaAs-OI waveguide at a wavelength of 1550 nm. We characterized our photon-pair source and obtained a generation efficiency of $a \approx 0.096 \times 10^{12}$ pairs/(s · W^2) and a coincidence rate of $\mu' \approx 1.109 \times 10^3$ pair/s/nm with a CAR over 120. This represents one of the highest pair generation efficiencies of an integrated quantum source through SFWM. In addition, for the first time, we explored the EGB of a waveguide source, demonstrating a bandwidth of 2.0 THz.

We envisage better rate performances by including on-chip inverse taper couplers. An improved coupling efficiency will, in turn, result in a higher brightness of the source. Moreover, the use of ring resonator structures can enhance the excitation field and further improve the generation efficiency. In addition, certain advancements on device fabrication, such as the reduction of surface roughness and successful sidewall passivation, can further decrease propagation losses [22]. These actions can reduce the current limitations for CAR and further boost the generation rate. Moreover, it should be noted that additional improvements on the dispersion design, i.e., obtaining β_2 values closer to zero, can enable the generation of wider EGBs. Consequently, our study demonstrates that due to its

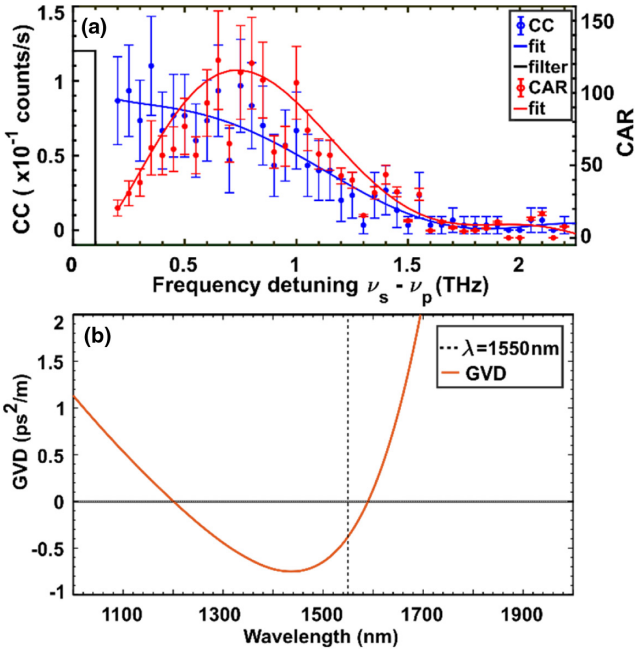

Fig. 3. (a) Measured coincidence counts (CCs) and coincidence-to-accidental ratio (CAR) as a function of pump-signal frequency detuning ($\nu_s - \nu_p$). The spectral blockage of the (notch filter) NF is illustrated schematically with a black line. Polynomial fits are included to guide the eye and $P_{\text{in}} = 354\ \mu\text{W}$. (b) Theoretical wavelength-dependent calculation of the group velocity dispersion (GVD) (β_2) of the fundamental quasi-TE mode. The GVD was calculated using a finite difference eigenmode (FDE) solver from the commercially available software (Lumerical, Inc.).

high photon-pair generation rate and broad emission bandwidth, AlGaAs-OI has a large potential to become an integrated platform for on-chip quantum communication and quantum information processing applications.

Funding. Engineering and Physical Sciences Research Council (EP/P005624/1); Bundesministerium für Bildung und Forschung (PQuMAL).

Acknowledgment. H. M., A. A., and M. K. acknowledge funding from the German federal ministry of education and research, Quantum Futur Program (PQuMAL). S. M. and M. S. acknowledge funding from the Engineering and Physical Sciences Research Council (EPSRC).

Disclosures. The authors declare no conflicts of interest.

REFERENCES

1. M. Krenn, M. Malik, T. Scheidl, R. Ursin, and A. Zeilinger, *Optics in Our Time* (Springer, 2016), pp. 455–482.
2. D. Bouwmeester, J. W. Pan, K. Mattle, M. Eibl, H. Weinfurter, and A. Zeilinger, Nature **390**, 575 (1997).
3. F. Flamini, N. Spagnolo, and F. Sciarrino, Rep. Prog. Phys. **82**, 016001 (2019).
4. H. J. Kimble, Nature **453**, 1023 (2008).
5. N. Sinclair, E. Saglamyurek, H. Mallahzadeh, J. A. Slater, M. George, R. Ricken, M. P. Hedges, D. Oblak, C. Simon, W. Sohler, and W. Tittel, Phys. Rev. Lett. **113**, 053603 (2014).
6. J. Lavoie, J. M. Donohue, L. G. Wright, A. Fedrizzi, and K. J. Resch, Nat. Photonics **7**, 363 (2013).
7. J. E. Sharping, K. F. Lee, M. A. Foster, A. C. Turner, B. S. Schmidt, M. Lipson, A. L. Gaeta, and P. Kumar, Opt. Express **14**, 12388 (2006).
8. M. Kues, C. Reimer, P. Roztocki, L. R. Cortés, S. Sciara, B. Wetzel, Y. Zhang, A. Cino, S. T. Chu, B. E. Little, D. J. Moss, L. Caspani, J. Azaña, and R. Morandotti, Nature **546**, 622 (2017).
9. X. Zhang, Y. Zhang, C. Xiong, and B. J. Eggleton, J. Opt. **18**, 074016 (2016).
10. C. Xiong, L. G. Helt, A. C. Judge, G. D. Marshall, M. J. Steel, J. E. Sipe, and B. J. Eggleton, Opt. Express **18**, 16206 (2010).
11. F. Boitier, A. Orieux, C. Autebert, A. Lemaître, E. Galopin, C. Manquest, C. Sirtori, I. Favero, G. Leo, and S. Ducci, Phys. Rev. Lett. **112**, 183901 (2014).
12. G. Maltese, M. I. Amanti, F. Appas, G. Sinnl, A. Lemaître, P. Milman, F. Baboux, and S. Ducci, npj Quantum Inf. **6**, 1 (2020).
13. C. Lacava, V. Pusino, P. Minzioni, M. Sorel, and I. Cristiani, Opt. Express **22**, 5291 (2014).
14. S. May, M. Kues, M. Clerici, and M. Sorel, Opt. Lett. **44**, 1339 (2019).
15. L. Chang, A. Boes, X. Guo, D. T. Spencer, M. J. Kennedy, J. D. Peters, N. Volet, J. Chiles, A. Kowligy, N. Nader, D. D. Hickstein, E. J. Stanton, S. A. Diddams, S. B. Papp, and J. E. Bowers, Laser Photon. Rev. **12**, 1800149 (2018).
16. H. K. Tsang, C. S. Wong, T. K. Liang, I. E. Day, S. W. Roberts, A. Harpin, J. Drake, and M. Asghari, Appl. Phys. Lett. **80**, 416 (2002).
17. P. Kultavewuti, E. Y. Zhu, L. Qian, V. Pusino, M. Sorel, and J. S. Aitchison, Opt. Express **24**, 3365 (2016).
18. P. Kultavewuti, V. Pusino, M. Sorel, and J. S. Aitchison, Opt. Lett. **40**, 3029 (2015).
19. N. Morais, I. Roland, M. Ravaro, W. Hease, A. Lemaître, C. Gomez, S. Wabnitz, M. De Rosa, I. Favero, and G. Leo, Opt. Lett. **42**, 4287 (2017).
20. M. Pu, L. Ottaviano, E. Semenova, and K. Yvind, Optica **3**, 823 (2016).
21. L. Ottaviano, M. Pu, E. Semenova, and K. Yvind, Opt. Lett. **41**, 3996 (2016).
22. L. Chang, W. Xie, H. Shu, Q. F. Yang, B. Shen, A. Boes, J. D. Peters, W. Jin, C. Xiang, S. Liu, G. Moille, S. P. Yu, X. Wang, K. Srinivasan, S. B. Papp, K. Vahala, and J. E. Bowers, Nat. Commun. **11**, 1331 (2020).
23. G. Moille, L. Chang, W. Xie, A. Rao, X. Lu, M. Davanço, J. E. Bowers, and K. Srinivasan, Laser Photon. Rev. **14**, 2000022 (2020).
24. S. May, M. Clerici, and M. Sorel, Sci. Rep. **11**, 2052 (2021).
25. E. Stassen, C. Kim, D. Kong, H. Hu, M. Galili, L. K. Oxenløwe, K. Yvind, and M. Pu, APL Photon. **4**, 100804 (2019).
26. E. J. Stanton, J. Chiles, N. Nader, G. Moody, N. Volet, L. Chang, J. E. Bowers, S. Woo Nam, and R. P. Mirin, Opt. Express **28**, 9521 (2020).
27. X. Li, P. L. Voss, J. E. Sharping, and P. Kumar, Phys. Rev. Lett. **94**, 053601 (2005).
28. S. Clemmen, A. Perret, S. K. Selvaraja, W. Bogaerts, D. van Thourhout, R. Baets, P. Emplit, and S. Massar, Opt. Lett. **35**, 3483 (2010).
29. K. Guo, E. N. Christensen, J. B. Christensen, J. G. Koefoed, D. Bacco, Y. Ding, H. Ou, and K. Rottwitt, Appl. Phys. Express **10**, 062801 (2017).
30. H. Takesue and K. Inoue, Opt. Express **13**, 7832 (2005).
31. P. Sarrafi, E. Y. Zhu, K. Dolgaleva, B. M. Holmes, D. C. Hutchings, J. S. Aitchison, and L. Qian, Appl. Phys. Lett. **103**, 251115 (2013).
32. Y. H. Kao, M. N. Islam, J. M. Saylor, R. E. Slusher, and W. S. Hobson, J. Appl. Phys. **78**, 2198 (1995).
33. J.-M. Lee, W.-J. Lee, M.-S. Kim, and J. J. Ju, J. Lightwave Technol. **37**, 5428 (2019).
34. S. Gehrsitz, F. K. Reinhart, C. Gourgon, N. Herres, A. Vonlanthen, and H. Sigg, J. Appl. Phys. **87**, 7825 (2000).
35. E. Brainis, Phys. Rev. A **79**, 023840 (2009).